ACS APPLIED MATERIALS & INTERFACES

Letter

www.acsami.org

Durable Plasmonic Cap Arrays on Flexible Substrate with Real-Time Optical Tunability for High-Fidelity SERS Devices

Hyelim Kang, Chul-Joon Heo, Hwan Chul Jeon, Su Yeon Lee, and Seung-Man Yang*

National Creative Research Initiative Center for Integrated Optofluidic Systems, Department of Chemical and Biomolecular Engineering, Korea Advanced Institute of Science and Technology, 335 Gwahangno, Yuseong-gu, Daejeon, 305-701, Korea

Supporting Information

ABSTRACT: Active tunable plasmonic cap arrays were fabricated on a flexible stretchable substrate using a combination of colloidal lithography, lift-up soft lithography, and subsequent electrostatic assembly of gold nanoparticles. The arrangement of the plasmonic caps could be tuned under external strain to deform the substrate in reversible. Real-time variation in the arrangement could be used to tune the optical properties and the electromagnetic field enhancement, thereby a proving a promising mechanism for optimizing the SERS sensitivity.

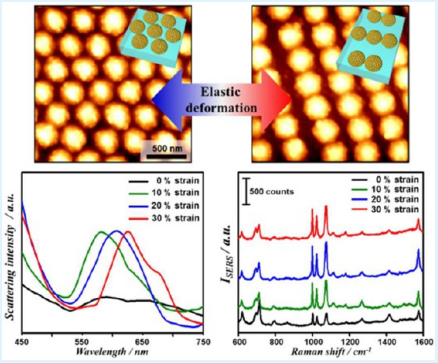

KEYWORDS: *colloidal lithography, surface-enhanced Raman scattering (SERS), flexible plasmonic substrate, optical tunability*

Raman scattering spectra have been used as molecular fingerprints to identify the presence of certain molecules. The Raman scattering intensity may be significantly amplified in the presence of plasmonic surface structures via the generation of enhanced electromagnetic (EM) fields due to surface plasmon resonance (SPR). Surface-enhanced Raman scattering (SERS) processes based on SPR have been widely used for the label-free molecular recognition of chemicals and biomolecules.[1] The SERS sensitivity depends strongly on the EM field enhancement induced from the surface plasmon. A plethora of studies have been conducted to optimize the surface patterns of arrayed metallic nanostructures. SPR can be tuned by adjusting the shape, size, composition, environment, and feature distance in the metal nanostructure arrays.[2−7] Among these properties, the feature distance is one of the most significant factors for SERS responses because the local EM field enhancement is amplified by coupling among adjacent metal nanostructures.[8−11] A variety of metal nanostructures, including aggregated metal colloids,[12] hole arrays,[13] and nanoparticle arrays[14] with controlled feature gap distances, have been suggested for use in high-fidelity SERS devices.

The systems studied previously have yielded only limited tunability with respect to the optical properties after fabrication of the SERS devices. The optical properties can generally be optimized (and are fixed) only for a specific range in the SPR spectrum during fabrication by preparing the arrays under tailored fabrication conditions. Recently, actively tunable plasmonic systems were developed using pH- and temperature-sensitive polymers[15−18] or stretchable polymers[7,19−25] as substrate materials to overcome the limitations on tunability. The feature gaps in the pH- and temperature-sensitive polymer films were controlled by swelling or shrinking the polymer matrix in response to an external stimulus. For example, a device may be immersed in an ionic solution or heated on a hot plate. Such systems may be restrictedly used in sensing applications not only because the responses are too slow to permit real-time tuning but also because the substrate conditions available for tuning the optical properties are limited. The plasmonic properties of the stretchable polymer substrate could be adjusted to a specific range by varying the intensity of the applied strain under ambient conditions. Thin metal films deposited onto a polymer substrate to form an array were found to crack easily in the stretched state.[21] Such properties must be avoided in practical applications to achieve reversibility. Despite recent advances, the fabrication of regular metal nanostructures on tunable substrates over a large area remains a challenge.[19]

Here, we demonstrate the preparation of highly active plasmonic cap arrays on a flexible substrate over a large area to achieve real-time optical tunability for SERS devices. Colloidal or nanosphere lithography is a robust and cost-effective route to the fabrication of uniformly ordered nanostructures in large area as compared with elaborating advanced lithography (e.g., e-beam lithography), which is a time-consuming technique and requires high cost instrumentation.[26−28] Furthermore, colloidal lithography enables to manipulate simply the feature scale and permits to fabricate readily complicated 3D structures. When

Received: January 2, 2013
Accepted: May 15, 2013
Published: May 15, 2013

   dx.doi.org/10.1021/am400019v | ACS Appl. Mater. Interfaces 2013, 5, 4569−4574

combined with other conventional lithographic techniques, this approach permits the preparation of a variety of nanostructures with novel features.[26,29] In this study, we used colloidal lithography in combination with lift-up soft lithography to obtain plasmonic cap arrays on a deformable substrate that acted as a hot spot to generate a strongly enhanced EM field. The plasmonic cap arrays consisted of self-assembled gold nanoparticles on a single layer of colloidal particle arrays that provided a template. Metal nanoparticles in the SERS structures only assembled on the surfaces of the colloidal particles, not on the deformable substrate; hence, crack formation problems in a metal film could be avoided. The result displayed a tunable plasmonic extinction ranging from 581 to 625 nm, depending on the external strain applied to the deformable substrate. Furthermore, the SERS signals could be optimized by mechanically manipulating the stretchable substrate to vary the gap distance between adjacent plasmonic caps. The optically active plasmonic cap arrays have potential for use as on-demand SERS platforms in which the elastic deformation of the substrate under mechanical manipulation provides plasmon tunability.

The plasmonic cap arrays were fabricated via colloidal lithography, combined with lift-up soft lithography and the subsequent electrostatic assembly of gold nanoparticles, as shown in Scheme 1. A hexagonally ordered single layer of silica

Scheme 1. Schematic Diagram Showing the Fabrication of the Plasmonic Cap Arrays on a Flexible Substrate[a]

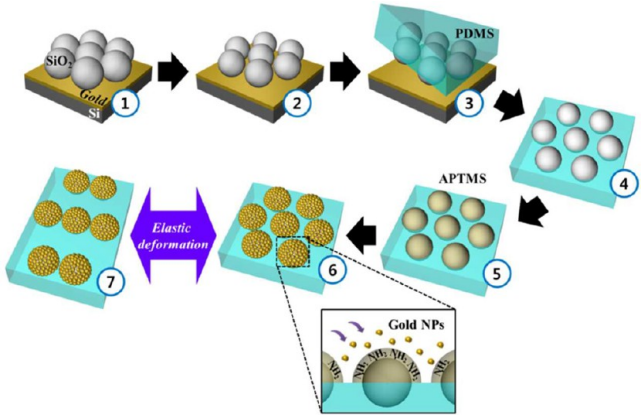

[a](1) Silica colloidal particles were spin-coated onto the as-prepared gold films to form a monolayer. (2) Reactive ion etching with CF_4 gas was performed to reduce the particle size. (3) The non-close-packed silica monolayer was transferred onto the PDMS substrate using lift-up soft lithography. (4) Partially embedded silica particles on the PDMS substrate. (5) Exposed silica surfaces were modified with APTMS molecules to provide a positive surface charge. (6) Plasmonic cap arrays on the PDMS substrate. The negatively charged gold nanoparticles were self-assembled on the modified silica surfaces via electrostatic interactions. (7) The plasmonic cap arrangement was tuned by the elastic deformation of the PDMS substrate in real time.

particles was prepared on a gold thin film by spin-coating a monodisperse colloidal suspension. Reactive ion etching (RIE) using CF_4 gas was then performed to reduce the particle size, resulting in nonclosely packed particle arrays (see the Supporting Information, Figure S1). The nanoparticle arrays were transferred onto the polydimethylsiloxane (PDMS) substrate using lift-up soft lithography that preserved the hexagonal ordering.[30,31] Uniformly ordered metallic nanostructures were easily fabricated on the elastomeric substrate over a large area because the transferred colloidal arrays served as templates for the metal nanoparticles.[32] The exposed surfaces of the transferred silica particles, which were partially embedded on the PDMS substrate, were functionalized with amine functional groups via the self-assembly of 3-aminopropyltrimethoxysilane layers.[33] Negatively charged gold nanoparticles were self-assembled on the amine-functionalized silica surfaces via electrostatic interactions to form highly ordered plasmonic cap arrays.[34] Finally, plasmonic cap arrays based on the PDMS substrate was fabricated with high uniformity in a large area (see the Supporting Information, Figure S2).

Figure 1a shows scanning electron microscopy (SEM) images of plasmonic cap arrays after gold nanoparticle assembly over deposition times ranging from 0 to 40 min. The domains of selectively assembled gold nanoparticles increased with the reaction time, and a full coverage of the cap structures was prepared after 40 min of assembly. The gold content within a fixed area of the silica particle varied as a function of the gold nanoparticle assembly time, as determined using energy dispersive spectrometry (EDS) and SEM, as shown in Figure 1b. The gold content gradually increased to 12.9 wt % with the reaction time. (The raw EDS data and the calculated elemental contents in the plasmonic cap arrays are shown in Figure S3 in the Supporting Information.) Figure 1c shows that the absorbance spectra of the plasmonic cap arrays were broadened and red-shifted due to the narrow distance between the assembled gold nanoparticles on the silica surfaces compared with gold nanoparticle suspension.[34] Plasmon coupling effects from the gold nanoparticles assembled on the silica surfaces caused a red shift in the absorbance peak as the deposition time was increased up to 30 min. Gold nanoparticles were fully assembled on the exposed surfaces after 30 min; hence, the absorbance spectrum observed after 40 min deposition was almost identical to that measured after 30 min deposition, even though the gold content increased (Figure 1b) becausee of the deposition of gold nanoparticles on the surfaces. Here, the sufficient deposition of gold nanoparticles was quite significant for preparing the tunable plasmonic cap arrays. In the present system, the network of gold nanoparticles on each silica sphere was aggregated with high density and finally formed like roughened film after 40 min. With this structure, the plasmonic effect from the crevices between assembled gold nanoparticles on each sphere was diminished and the plasmonic effect solely from the arrangement of plasmonic caps became dominated.[32] The dominant contribution from the gaps between neighboring plasmonic caps to the enhanced plasmonic response was confirmed by measuring the Raman signals from the various substrates which were prepared in different gold nanoparticle assembly times. Furthermore, the network of gold nanoparticles on each sphere could generate more enhanced EM field than the continuous metal-coated sphere.[35]

In this system, control over the nanosized gap distance between adjacent plasmonic caps was achieved by modulating the external strain on the elastomer substrate. The optical extinction of the plasmonic caps could be tuned by applying strain to the substrate, even after the array preparation steps. Figure 2a shows atomic force microscopy (AFM) images of the plasmonic cap arrays under various strains applied to the substrates. The percentage of the strain was calculated by measuring changes in the total length of the PDMS substrate before or after deformation. The interparticle distance between plasmonic caps could be tuned by the elastic deformation of the

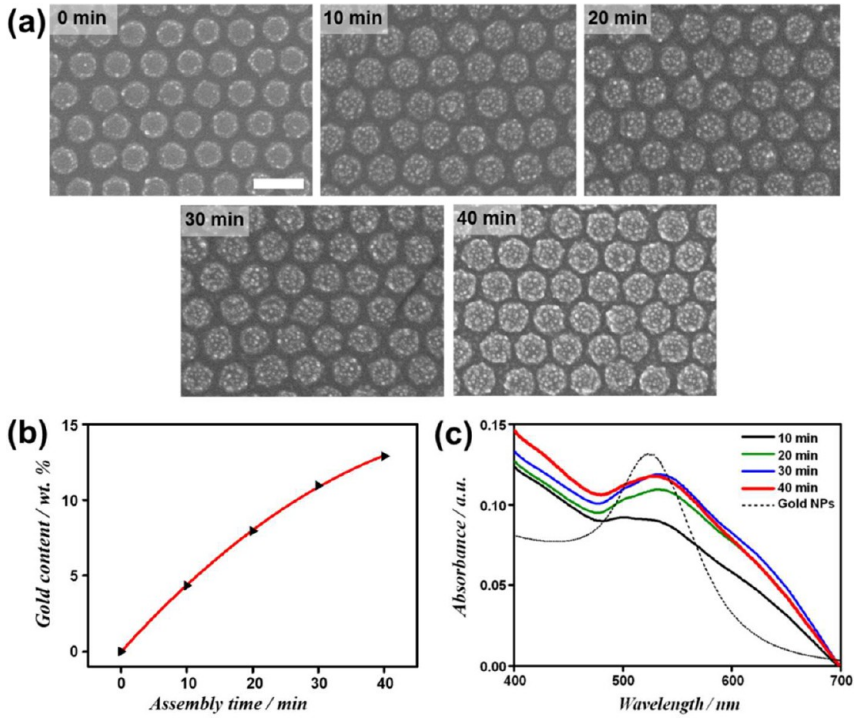

Figure 1. (a) SEM images of the plasmonic cap arrays created by the electrostatic self-assembly of gold nanoparticles on the APTMS-modified silica surfaces with varying assembly times, from 0 to 40 min. (b) Variations in the gold content in the plasmonic cap arrays as a function of the gold nanoparticle assembly time. (c) Optical properties of the gold nanoparticle suspension and the plasmonic cap arrays as a function of the assembly time. The scale bar indicates 500 nm.

PDMS substrate. When the plasmonic substrate was elongated by external strain, such spacings inhomogeneously changed depending on the angle of the plasmonic cap relative to the strain axis.[36] The plasmonic caps remained closely aligned along the direction perpendicular to the applied strain, whereas the gap distance between adjacent plasmonic caps along the other direction in the hexagonal array became broader (Figure 2a).[36] As a result, the dimensions of the plasmonic cap array changed from a hexagonal arrangement (under 0% strain) to a one-dimensional array of particle chains (under 30% strain). These reduced gap distance and increased gap distance were defined as G_1 and G_2 for convenience. Panels b and c in Figure 2 show the values of G_1 and G_2, calculated on the basis of the AFM images (see the Supporting Information, Figure S4). G_1 was tuned between 80 and 34 nm, and G_2 was tuned between 80 and 127 nm under a 30% strain. As shown in Figure 2b, the value of G_1 was converged ~30 nm because silica spheres were partially embedded in PDMS matrix that prevented touching each metallic caps.[37] On the contrary, the value of G_2 was gradually increased during elongation process (Figure 2c). When the plasmonic substrate was suffered from 30% or higher strain, the distance between closely aligned caps was kept ~30 nm long, with a gradual increase in the distance between neighboring one-dimensional particle chain. The resonance wavelength, which depended strongly on the arrangement of the metallic nanostructures,[38,39] could be tuned by controlling the distances between the plasmonic caps. The local plasmonic properties were characterized under the external strain by measuring the scattering from the plasmonic cap arrays using a dark-field microscope equipped with a spectrometer. The hexagonally ordered plasmonic caps with uniform spacings between adjacent caps exhibited a resonance wavelength at 581 nm. As G_1 decreased, the resonance wavelength became red-shifted from 581 to 625 nm because of the plasmonic coupling effects with plasmonic caps several tens of nanometers in length, as shown in Figure 2d. Furthermore, the scattering intensity, which had a similar trend to the value of G_1, was increased evidently with the strain as large as 10% due to plasmonic coupling effect like a pair of nanoparticles.[40,41] These results confirmed that the optical properties could be easily adjusted in real-time by controlling the applied strain, thereby tuning the arrangement of the plasmonic caps.

The plasmonic cap arrays were expected to display a highly enhanced EM field arising from the aggregated gold nanoparticles on the individual caps and the interparticle coupling from the plasmonic caps separated by nanoscale gaps. The real-time optical tunability of the resulting plasmonic cap arrays may potentially be used to design a tunable SERS platform. A SERS application was demonstrated by immersing a plasmonic cap array in a 1 μM benzenethiol (BT) solution for 1 h for immobilization on the gold surfaces. The Raman signals of BT, which has characteristic peaks at 994, 1017, 1071, and 1571 cm^{-1},[42] were measured under various substrate strain values to verify the arrangement effects on the EM field enhancement at specific optical frequencies, as shown in Figure 3. The intensity of the Raman signals obtained from the substrate clearly changed depending on the arrangement of the plasmonic caps (Figure 3a). As the applied strain increased from 0 to 30%, the SPR resonance wavelength was red-shifted toward laser excitation wavelength (632.8 nm), which led to a stronger EM field. As a matter of fact, however, the complicated combination and competition between inhomogeneous spacings (G_1 and G_2) have a decisive effect for the enhanced Raman signals in the present system. The value of G_2 increased resulting in a weaker plasmon coupling effect derived from the defunctionalization as "hot spots".[43] A strong SERS signal,

dx.doi.org/10.1021/am400019v | ACS Appl. Mater. Interfaces 2013, 5, 4569−4574

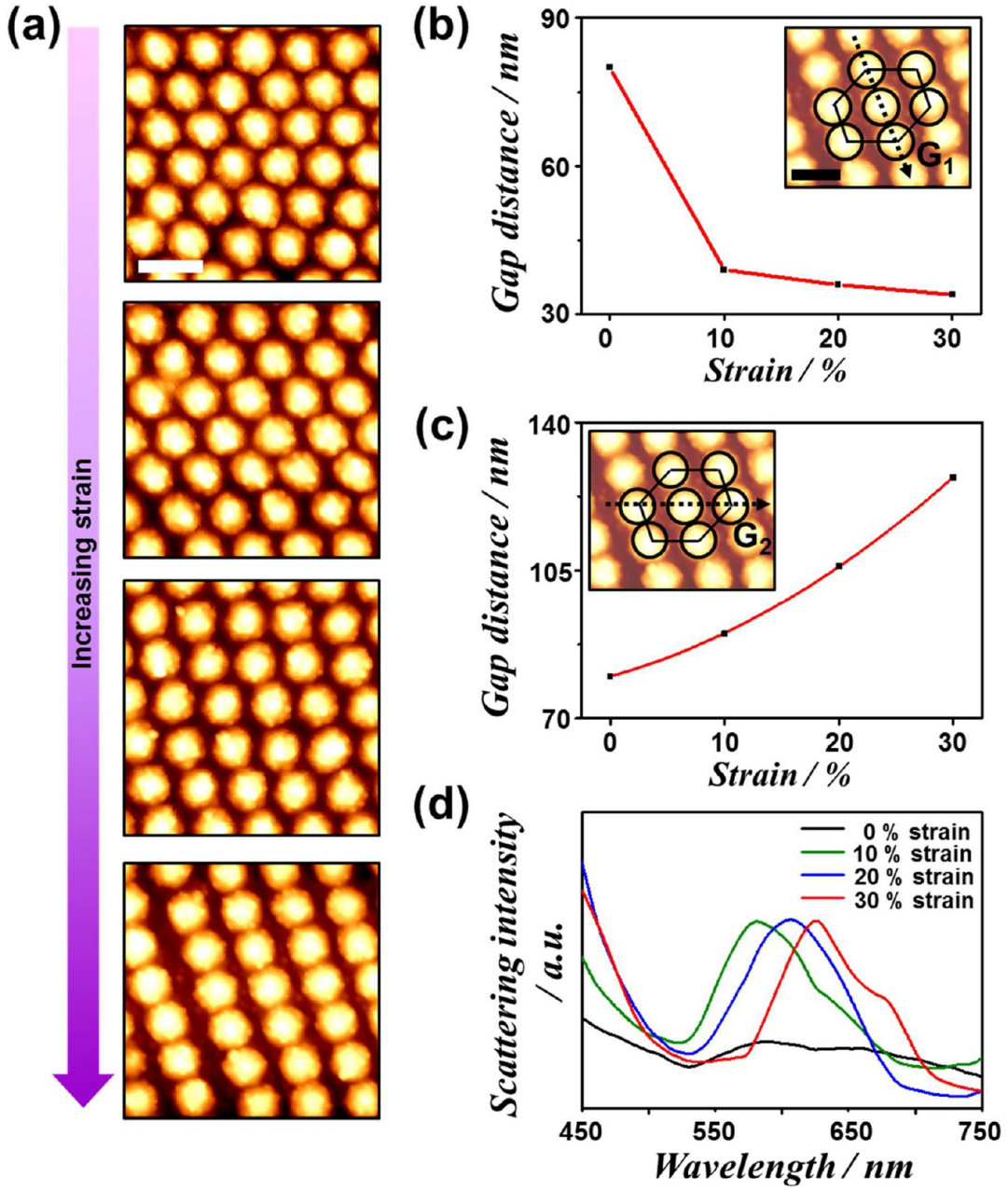

Figure 2. Tunable plasmonic cap arrays. (a) AFM images of the plasmonic cap arrays under various applied strains (0, 10, 20, and 30% strain). Variations in the gap distance between adjacent gold caps (b) perpendicular to the direction of applied strain (G_1) and (c) other gap distance in the hexagonal array (G_2). (d) Scattering spectra of the plasmonic cap arrays corresponding to the AFM images of (a). The scale bar indicates 500 nm.

attributed to the EM field, was enhanced across the activated nanogaps between adjacent plasmonic caps. The EM field enhancement due to the small nanogaps was particularly dominant compared with the isolated nanostructures in the SERS application.[43] Hence, the SERS sensitivity gradually increased, and was maximized when the substrate suffered from a 20% strain because of the optimized combined effects of the position of the structural resonance wavelength and the arrangement of the plasmonic caps. When the substrate was further extended (over a 20% strain), the widened G_2 (a value of 127 nm) was not narrow enough to perform as strong "hot spots" in SERS applications. Under this condition, the narrower G_1 became responsible for the enhanced Raman signals.[43] Finally, the SERS intensity decreased when the substrate was deformed under a strain exceeding 30% strain, compared with the 20% elongated sample, because the EM field due to G_2 decreased as these structures ceased to form "hotspots".

To determine that the high SERS sensitivity of the tunable plasmonic substrate resulting from changes in the nanostructure arrangement, a set of control experiments were performed in which the enhancement factors (EFs) from a substrate without strain were compared for various concentrations of a BT solution, as shown in Figure 3b. The SERS EF at 1017 cm^{-1} was calculated by comparing the signal intensities measured from the BT-adsorbed plasmonic substrates to intensities measured for the 99% BT solution onto a glass substrate as a reference (see the Supporting Information). The EF of BT (1 μM) could be increased to 7.102×10^3 in a plasmonic substrate under 20% strain, up from 2.373×10^3 for the as-prepared substrate. The error bars (Figure 3b) show a small fluctuation

dx.doi.org/10.1021/am400019v | ACS Appl. Mater. Interfaces 2013, 5, 4569−4574

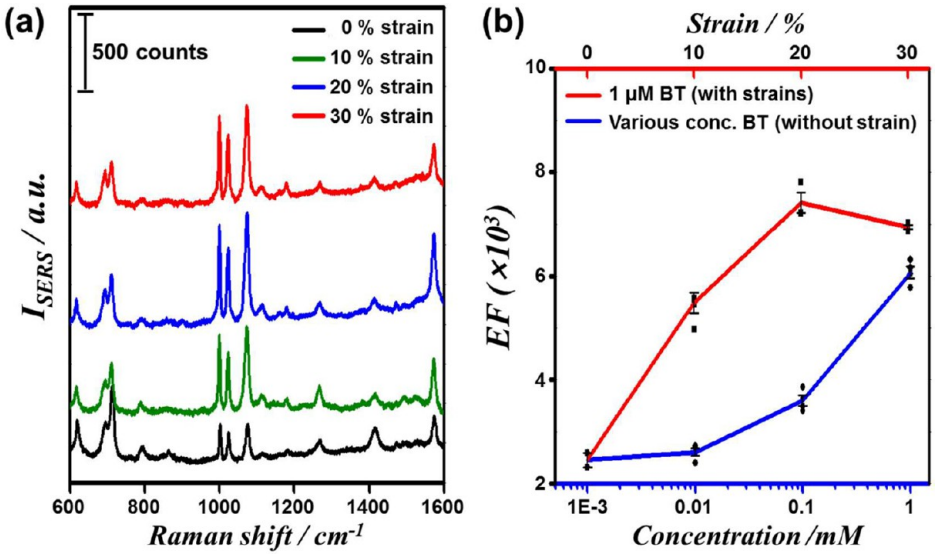

Figure 3. (a) Tunable SERS spectra of the 1 μM BT-adsorbed plasmonic cap arrays as a function of the applied strain. (b) Comparison of the enhancement factor (EF) from the tunable SERS signals in (a) and the SERS signals derived from the plasmonic cap arrays without external strain, for various concentrations of BT.

of EFs at each elongated state, however, that is a negligible change. When the substrate was elongated, EF increased more than 3 times in the same analyte of equal concentration. It is noteworthy that the maximal EF, which occurred from the 20% elongated plasmonic substrate (at 1 μM BT case), exceeded the value obtained from a sample, prepared using a 1000-fold higher concentration (1 mM) of the BT solution, without deforming the substrate (Figure 3b). Consequently, it was confirmed that the small change in the stretchable substrate, which induced rearrangement of the plasmonic caps, could be much more efficient approach for enhancing the SERS intensity rather than a 1000-fold increase in the analyte concentration. Furthermore, by using the 20% elongated plasmonic substrate, BT concentration as low as 10 nM, which was an lower limit of detection (LOD) for the normal-stated plasmonic cap arrays, could be detected in a reproducible manner (see the Supporting Information, Figure S5). Indeed, improved LOD with 100-fold enhanced SERS sensitivity could be obtained from the stretched substrate compared with the original substrate. Also, the scattering peak position could be tuned in reversible and repeatable manner without appreciable deviations during cyclic mechanical manipulation (see the Supporting Information, Figure S6). The gold nanoparticles on each silica sphere were maintained and the arrangement of plasmonic cap arrays was successfully recovered without any fracture after several times of SERS tunability tests (see the Supporting Information, Figure S6). Therefore, our tunable plasmonic cap arrays showed potential as excellent durable SERS substrates, even under extreme dilution conditions.

In conclusion, we demonstrated the preparation of active plasmonic cap arrays on a flexible substrate that provided real-time optical tunability for use as an effective SERS sensor. The uniform plasmonic cap arrays were fabricated over a large area via colloidal lithography combined with lift-up soft lithography and the electrostatic assembly of gold nanoparticles. The optical properties and SERS sensitivities could be tuned in real time using a single plasmonic substrate. Furthermore, the SERS signals could be intensified by controlling the arrangement of the plasmonic caps, resulting in additional EM field enhancements due to the nanogaps. Small change (20% strain) in the stretchable plasmonic substrate was much more effective in enhancing the SERS intensity than a 1000-fold increase in the analyte concentration as obtained at zero strain. The plasmonic cap arrays, which were composed of biocompatible materials, may potentially be used not only as patch-type SERS devices using the flexibility but also as an on-demand SERS platform in a microfluidic chip for a biomolecular sensing probe.[44]

■ ASSOCIATED CONTENT

Ⓢ Supporting Information

The experimental method and SERS analysis details. This material is available free of charge via the Internet at http://pubs.acs.org.

■ AUTHOR INFORMATION

Corresponding Author

*E-mail: smyang@kaist.ac.kr. Tel.: +82-42-350-3962. Fax: +82-42-350-5962.

Notes

The authors declare no competing financial interest.

■ ACKNOWLEDGMENTS

This work has been supported by a grant from the Creative Research Initiative Program of the Ministry of Education, Science and Technology for "Complementary Hybridization of Optical and Fluidic Devices for Integrated Optofluidic Systems". This research has been supported by WCU (World Class University) program through the National Research Foundation of Korea funded by the Ministry of Education, Science and Technology (*R*32-2008-000-10142-0). The authors also appreciated partial support from the Brain Korea 21 Program.

■ REFERENCES

(1) Li, J. F.; Huang, Y. F.; Ding, Y.; Yang, Z. L.; Li, S. B.; Zhou, X. S.; Fan, F. R.; Zhang, W.; Zhou, Z. Y.; Wu, D. Y.; Ren, B.; Wang, Z. L.; Tian, Z. Q. *Nature* **2010**, *464*, 392−395.

(2) Murray, W. A.; Barnes, W. L. *Adv. Mater.* **2007**, *19*, 3771−3782.

(3) Anker, J. N.; Hall, W. P.; Lyandres, O.; Shah, N. C.; Zhao, J.; Van Duyne, R. P. *Nat. Mater.* **2008**, *7*, 442−453.
(4) Mock, J. J.; Barbic, M.; Smith, D. R.; Schultz, D. A.; Schultz, S. *J. Chem. Phys.* **2002**, *116*, 6755−6759.
(5) Heo, C. J.; Kim, S. H.; Jang, S. G.; Lee, S. Y.; Yang, S. M. *Adv. Mater.* **2009**, *21*, 1726−1731.
(6) Ye, J.; Wen, F.; Sobhani, H.; Lassiter, J. B.; Van Dorpe, P.; Nordlander, P.; Halas, N. J. *Nano Lett.* **2012**, *12*, 1660−1667.
(7) Di Falco, A.; Ploschner, M.; Krauss, T. F. *New J. Phys.* **2010**, *12*, 113006.
(8) Acimovic, S. S.; Kreuzer, M. P.; Gonzalez, M. U.; Quidant, R. *Acs Nano* **2009**, *3*, 1231−1237.
(9) Yan, B.; Thubagere, A.; Premasiri, W. R.; Ziegler, L. D.; Dal Negro, L.; Reinhard, B. M. *Acs Nano* **2009**, *3*, 1190−1202.
(10) Tao, A.; Sinsermsuksakul, P.; Yang, P. *Nat. Nanotechnol.* **2007**, *2*, 435−440.
(11) Heo, C.-J.; Jeon, H. C.; Lee, S. Y.; Jang, S. G.; Cho, S.; Choi, Y.; Yang, S.-M. *J. Mater. Chem.* **2012**, *22*, 13903.
(12) Zhu, Z. H.; Zhu, T.; Liu, Z. F. *Nanotechnology* **2004**, *15*, 357−364.
(13) Yu, Q. M.; Guan, P.; Qin, D.; Golden, G.; Wallace, P. M. *Nano Lett.* **2008**, *8*, 1923−1928.
(14) Wang, H. H.; Liu, C. Y.; Wu, S. B.; Liu, N. W.; Peng, C. Y.; Chan, T. H.; Hsu, C. F.; Wang, J. K.; Wang, Y. L. *Adv. Mater.* **2006**, *18*, 491−495.
(15) Lu, Y.; Liu, G. L.; Lee, L. P. *Nano Lett.* **2005**, *5*, 5−9.
(16) Gupta, M. K.; Chang, S.; Singamaneni, S.; Drummy, L. F.; Gunawidjaja, R.; Naik, R. R.; Tsukruk, V. V. *Small* **2011**, *7*, 1192−1198.
(17) Qian, X. M.; Li, J.; Nie, S. M. *J. Am. Chem. Soc.* **2009**, *131*, 7540−7541.
(18) Housni, A.; Zhao, Y. *Langmuir* **2010**, *26*, 12366−12370.
(19) Alexander, K. D.; Skinner, K.; Zhang, S. P.; Wei, H.; Lopez, R. *Nano Lett.* **2010**, *10*, 4488−4493.
(20) Olcum, S.; Kocabas, A.; Ertas, G.; Atalar, A.; Aydinli, A. *Opt. Express* **2009**, *17*, 8542−8547.
(21) Cole, R. M.; Mahajan, S.; Baumberg, J. J. *Appl. Phys. Lett.* **2009**, *95*, 154103.
(22) Aksu, S.; Huang, M.; Artar, A.; Yanik, A. A.; Selvarasah, S.; Dokmeci, M. R.; Altug, H. *Adv. Mater.* **2011**, *23*, 4422−4430.
(23) Zhu, X. L.; Shi, L.; Liu, X. H.; Zi, J.; Wang, Z. L. *Nano Res.* **2010**, *3*, 807−812.
(24) Huang, F. M.; Baumberg, J. J. *Nano Lett.* **2010**, *10*, 1787−1792.
(25) Pryce, I. M.; Aydin, K.; Kelaita, Y. A.; Briggs, R. M.; Atwater, H. A. *Nano Lett.* **2010**, *10*, 4222−4227.
(26) Yang, S. M.; Jang, S. G.; Choi, D. G.; Kim, S.; Yu, H. K. *Small* **2006**, *2*, 458−475.
(27) Lee, S. Y.; Kim, S. H.; Jang, S. G.; Heo, C. J.; Shim, J. W.; Yang, S. M. *Anal. Chem.* **2011**, *83*, 9174−9180.
(28) Vogel, N.; Weiss, C. K.; Landfester, K. *Soft Matter* **2012**, *8*, 4044−4061.
(29) Lee, S. Y.; Kim, S. H.; Heo, C. J.; Hwang, H.; Yang, S. M. *Phys. Chem. Chem. Phys.* **2010**, *12*, 11861−11868.
(30) Yao, T. J.; Wang, C. X.; Lin, Q.; Li, X.; Chen, X. L.; Wu, J.; Zhang, J. H.; Yu, K.; Yang, B. *Nanotechnology* **2009**, *20*, 065304.
(31) Li, X.; Wang, T. Q.; Zhang, J. H.; Yan, X.; Zhang, X. M.; Zhu, D. F.; Li, W.; Zhang, X.; Yang, B. *Langmuir* **2010**, *26*, 2930−2936.
(32) Jang, S. G.; Choi, D. G.; Heo, C. J.; Lee, S. Y.; Yang, S. M. *Adv. Mater.* **2008**, *20*, 4862−4867.
(33) Jang, S. G.; Kim, S. H.; Lee, S. Y.; Jeong, W. C.; Yang, S. M. *J. Colloid Interface Sci.* **2010**, *350*, 387−395.
(34) McConnell, M. D.; Kraeutler, M. J.; Yang, S.; Composto, R. J. *Nano Lett.* **2010**, *10*, 603−609.
(35) Cho, W. J.; Kim, Y.; Kim, J. K. *Acs Nano* **2012**, *6*, 249−255.
(36) Millyard, M. G.; Huang, F. M.; White, R.; Spigone, E.; Kivioja, J.; Baumberg, J. J. *Appl. Phys. Lett.* **2012**, *100*, 073101.
(37) Fudouzi, H.; Sawada, T. *Langmuir* **2006**, *22*, 1365−1368.
(38) Jeon, H. C.; Heo, C. J.; Lee, S. Y.; Park, S. G.; Yang, S. M. *J. Mater. Chem.* **2012**, *22*, 4603−4606.
(39) Jiang, L.; Sun, Y. H.; Nowak, C.; Kibrom, A.; Zou, C. J.; Ma, J.; Fuchs, H.; Li, S. Z.; Chi, L. F.; Chen, X. D. *Acs Nano* **2011**, *5*, 8288−8294.
(40) Reinhard, B. M.; Siu, M.; Agarwal, H.; Alivisatos, A. P.; Liphardt, J. *Nano Lett.* **2005**, *5*, 2246−2252.
(41) Liu, G. L.; Yin, Y. D.; Kunchakarra, S.; Mukherjee, B.; Gerion, D.; Jett, S. D.; Bear, D. G.; Gray, J. W.; Alivisatos, A. P.; Lee, L. P.; Chen, F. Q. F. *Nat. Nanotechnol.* **2006**, *1*, 47−52.
(42) Hwang, H.; Kim, S. H.; Yang, S. M. *Lab Chip* **2011**, *11*, 87−92.
(43) Gunnarsson, L.; Bjerneld, E. J.; Xu, H.; Petronis, S.; Kasemo, B.; Kall, M. *Appl. Phys. Lett.* **2001**, *78*, 802−804.
(44) Tao, H.; Brenckle, M. A.; Yang, M. M.; Zhang, J. D.; Liu, M. K.; Siebert, S. M.; Averitt, R. D.; Mannoor, M. S.; McAlpine, M. C.; Rogers, J. A.; Kaplan, D. L.; Omenetto, F. G. *Adv. Mater.* **2012**, *24*, 1067−1072.